Part I: Characteristics of Coastal Waves and Currents

Wave Diffraction E of Hornbæk Harbour, Zealand

North Sea Waves at Groin Protected Danish West Coast

The modelling of a spilling breaker: strong turbulence at a free surface.

M. Brocchini † and D.H. Peregrine ‡

Abstract

A brief review is given of the initial development of a model for the turbulence generated by a spilling breaker riding on an unsteady wave. The turbulent volume of water in a spiller is modelled as a thin layer. The basis for such a model comes from the analysis of the interaction between an air-water interface with patche of turbulence. Hence, the behaviour of a free surface which is affected by strong turbulence is being studied. We summarise some of the salient points of our work. These include a derivation of averaged boundary conditions which include mass and momentum flows in the surface layer and the transfer to the bulk liquid. A brief account is also given of the type of equations needed to represent the motion of the front edge of the breaker. Illustration of the method is only given in terms of the equations derived by integration from the equation of mass conservation. Finally, there is description of the various free surface regimes that occur and need to be considered in order to determine suitable closures for the averaged terms.

Motivation and Methodology

This study is motivated by a wish to model the spilling breakers that arise from the crests of steep water waves (e.g. see figure 1). Spilling breakers are classified in a wider class of types of breaking where the wave form changes relatively slowly. Together with the bore (or turbulent bore) they form the class of the quasi-steady breakers. If the turbulence is confined to a region near the crest of the wave the wave is a spilling breaker but if the whole face of the wave is turbulent it is a bore.

In their analysis of spilling breakers, bores and hydraulic jumps Peregrine & Svendsen (1978) suggested that the volume of turbulent flow in a spilling breaker resembles a turbulent mixing layer. The roller model in which the turbulent

†Assistant Professor, Istituto di Idraulica, Universitá di Genova, Via Montallegro 1, 16145 Genova, Italy, (*brocchin@idra.unige.it*)

‡Professor of Applied Mathematics, School of Mathematics, University of Bristol, (*D.H.Peregrine@bristol.ac.uk*)

region is modeled as a separate flow region passively riding the wave crest is seen to be only a partial solution as it is evident that the fluid content of the roller itself is continually mixing with the rest of the turbulent fluid in the wave.

Peregrine (1992) also suggests that a spilling breaker may be considered as a quasi-steady system in a frame of reference moving with the wave where deformations of the spiller shape occur at longer time scales than those typical of the motion of water through the turbulent region. The structure of such a quasi-steady breaker is thus an initial mixing layer region, followed by a region beneath the crest of the wave where gravity influences and restrains the turbulent motions near the surface.

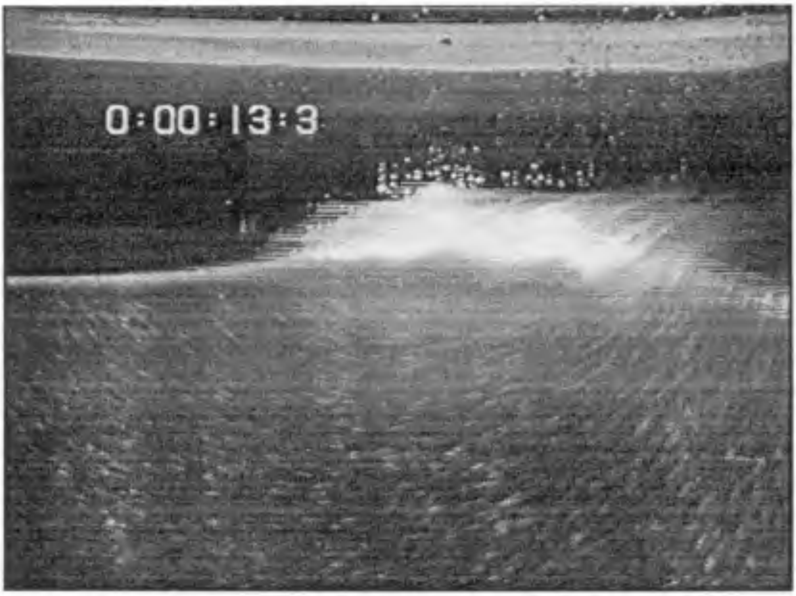

Figure 1: Example of a spilling breaker. Photograph taken at the Fluid Dynamics unit of the University of Edinburgh. (Courtesy of T.C.D. Barnes.)

Developing some of the ideas suggested in Peregrine & Svendsen (1978) and Peregrine (1992) we are trying to build a model which is:

1. as *reliable* and *accurate* as possible in terms of numerical solver $\Longrightarrow$ use a boundary integral solver for the irrotational flow of the bulk of the breaking wave (for a detailed description please refer to Dold & Peregrine, (1984) and Cooker *et al* (1990);

2. as *complete* as possible in terms of physical phenomena $\Longrightarrow$ take into account: two-phase flow, turbulence, flow unsteadiness and curvature, response of turbulence to curvature ...;

3. as *simple* as possible $\Longrightarrow$ lump the effects of two-phase and turbulent flow into Boundary Conditions for the solver used to model the bulk of the propagating wave.

[for more details on this model we refer the reader to Brocchini (1996).]

As a result we are working at a 'three-layer-model' a sketch of which is reported in figure 2. Note that in this model three different time scales are of relevance. They are respectively the time scale for the water particles to cross the layer, the time scale for the evolution of the layer shape and the time scale for the evolution of the shape of the underlying wave. Even if the spilling breaker is said to be quasi-steady because its evolution occurs at a larger time scale than that for a particle to cross the layer, it can be considered unsteady when referring to the motion of the wave because the evolution of the wave shape occurs at a larger time scale than the evolution of the thin layer.

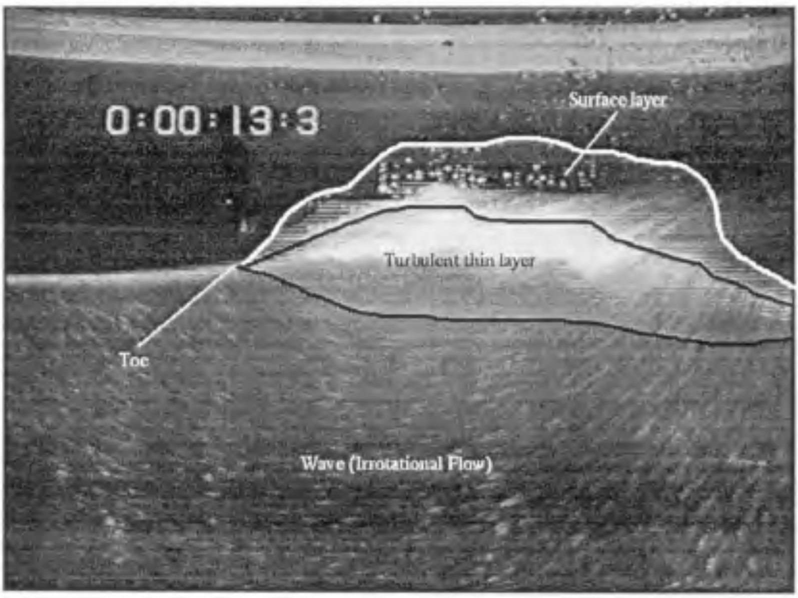

Figure 2: Global geometry adopted in the model for the system wave - turbulent thin layer - surface layer.

One of the main difficulties in modelling a spilling breaker is that at present there is no good description of free surface boundary conditions for a turbulent flow. The most interesting, and difficult, flows are those breakers which are strongly nonlinear and splashing, but even the much smoother flows occurring in small "micro-scale" breakers, that are restrained by surface tension, require special attention. Hasselmann (1971) is the only paper we know that describes similar surface flows in the context of both wave and turbulent averaging.

In that paper a perturbation is made about the undisturbed free surface, assuming Taylor series make good approximations. This may be a good approximation for irrotational motions but is clearly more limited for turbulence. An interaction stress tensor and a surface mass transfer must be introduced to take proper account of interactions between short and long period motions. However this particular analysis is no longer appropriate when turbulent eddies cause the interface to develop sharply curved features or to disintegrate into splashes. In this case the problem to be faced is of a twofold nature as both turbulence and two-phase flow must be taken into account (e.g. see top layer of figure 2). The interface between the air and water can be extremely complex.

Here we only analyse the problems of modelling the top layer ('surface layer'). At first we illustrate the physical/mathematical framework which concerns both the avaraging within the two-phase layer and the subsequent definition of suitable model equations and boundary conditions. Then, a brief account is given on the equations which are needed to represent the motion of the front edge of the breaker ('toe of the breaker'). Finally, in recognition of the need for closures which depend on specific flow regimes, we describe the main features of such regimes leaving open (for moment) the question of quantifying closures.

The boundary conditions for the 'surface layer'.

The top region of the spilling breaker is studied as a layer consisting of an air-water mixture ('surface layer' of figure 3). The analysis of the flow of two fluids, one dispersed throughout the other, is most often carried out by solving equations which arise from averaging over each phase. In recent research this is achieved by introducing a 'phase function' or 'intermittency function', which is essentially a step function, and then averaging (e.g. Drew, 1983). The properties of the phase function are such that a number of conservation equations are obtained for each dispersed phase.

Within the layer flow properties (e.g. velocities) are not continuous functions of time and space hence we introduce a 'phase function' or 'intermittency function' such that:

$$I(s,n,t) = \begin{cases} 1 & \text{if } (s,n) \text{ is in the water at time } t \\ 0 & \text{if } (s,n) \text{ is in the air at time } t. \end{cases} \tag{1}$$

The we introduce an averaging process $\langle\cdot\rangle$ such that if $\mathcal{G}(s,n,t)$ is a generic flow variable then $\langle\mathcal{G}(s,n,t)\rangle = G(s,n,t)$ is the corresponding average. The most appropriate averaging process is the 'ensemble average' however many of the flows studied in the laboratory are statistically stationary with respect to time. If this is so, the ergodic hypothesis asserts that the time average is equivalent to the ensemble average and $\langle\cdot\rangle$ can simply be regarded as a time average.

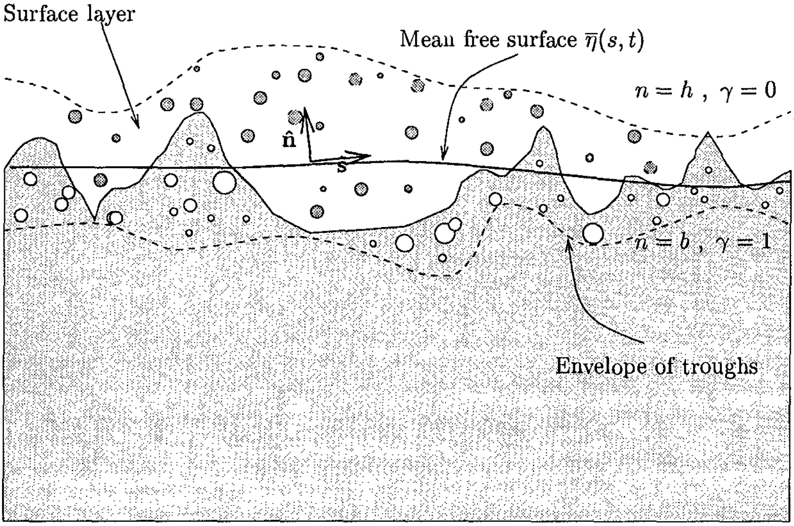

Figure 3: Global geometry adopted in the model for the surface layer.

After averaging the intermittency function becomes an average volume fraction $\gamma(s,n,t)$ also called 'intermittency factor' such that

$$\gamma(s,n,t) = \langle I(s,n,t) \rangle = \begin{cases} 1 & \text{below trough level } n = b \\ 0 & \text{above crest level } n = h. \end{cases} \tag{2}$$

Within the surface layer there can be regions in which only the air, or only the water, or both, are connected. Whether connected or not there is a range of γ from 0 to 1. Somewhere within the layer a mean interface can be defined. Several possible definitions are available, e.g. the surface $\gamma = 0.5$, or the surface corresponding to an equi-distribution, within the surface layer, of the two phases on each side of the chosen surface (see figure 3). In principle this interface can be regarded as a local reference for defining the origin of a local curvilinear coordinate set (s, n), where s follows the mean surface and n is normal to it. However, following experience developed in defining mean shorelines for waves on a beach (Brocchini & Peregrine, 1996) we choose to avoid any specific definition of the mean surface since it seems more meaningful to deal with the surface layer as a whole. For interaction with the water below, the lower boundary of the layer is most relevant, this we denote as b.

Since the intermittency factor γ is a continuous function of time and space it is most useful to characterize different flow conditions. For example three cases are here reported of a wavy surface (figure 4a), a 'scarified' surface (figure4b) and a splashing surface. This has been modelled by considering a Normal distribution

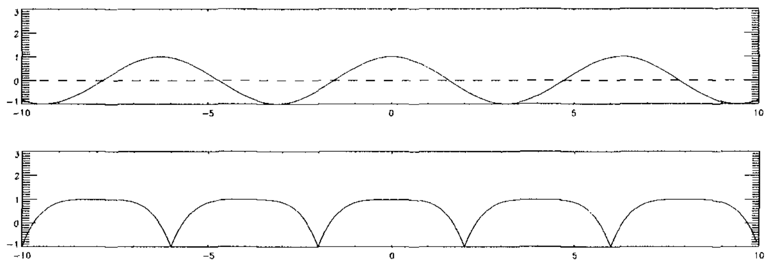

Figure 4: Free surface profile for: (a) sinusoidal wavy interface, (b) periodic scarified interface.

for η such that a simple result is obtained for γ:

$$\gamma(s,n,t) = \tfrac{1}{2}\left[1 - \mathrm{erf}\left(\frac{n-\overline{\eta}(s,t)}{\sqrt{2}\sigma(s,t)}\right)\right]. \tag{3}$$

[In this model σ is a measure of the lateral extent of the surface layer].

For each of the three types of surfaces we have a different γ factor which is reported in figure 5.

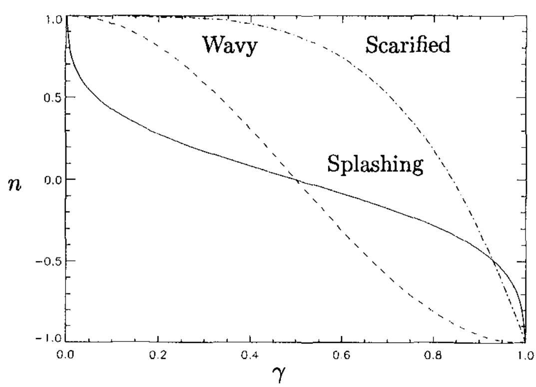

Figure 5: The intermittency factor (or residence time) γ for: (a) wavy air-water interface (dashed line), (b) periodically scarified interface (dot-dashed line) and (c) turbulent splashing interface (solid line).

It is evident that for wavy regimes water is present at the top of the surface layer ($n = 1$) for a longer time than for a splashing regime in which water drops are present for a shorter time near the top of the layer. This behaviour is reversed at the bottom of the layer where large values of γ ($\gamma \approx 1$) are reached faster while approaching the base of the layer ($n = -1$) in a splashing regime. The relative residence time is nearly 1 for most of a periodic scarified air-water interface.

In order to obtain the boundary conditions use the following steps:

1. obtain conservation equations using integral equations within a control volume V (for more details see Brocchini & Peregrine, (1998b)). With this method there is no need to rely on the usual assumption that each phase can be considered as a continuum;

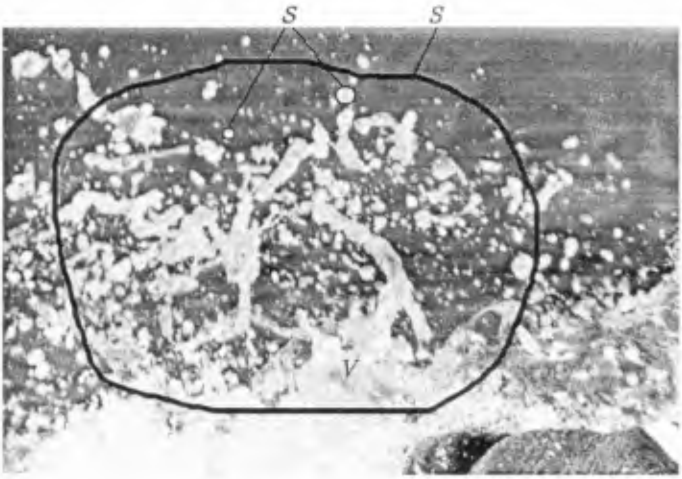

Figure 6: The air-water continuum. The thick closed curve represents the boundary S of the fixed control volume V. An example of the discontinuity interface $\mathcal{S}$ between the two phases is drawn around two water droplets.

2. for simplicity in initial studies assume air flow has negligible effect and no phase change occurs;

3. integrate conservation equations across the 'surface layer' i.e. from the base level $n = b(s,t)$ to crest level $n = h(s,t)$;

4. define the amount of water contained in the layer as:

$$d(s,t) \equiv \int_b^h \gamma \, dn. \tag{4}$$

To get the required boundary conditions we apply the above procedure to each conservation equation (i.e. conservation of mass, linear momentum ...).

For example application to the conservation of mass gives the following kinematic boundary condition:

$$\frac{\partial b}{\partial t} + U|_b \frac{\partial b}{\partial s} - V|_b = W = -\left(\frac{\partial d}{\partial t} + \frac{\partial}{\partial s}\int_b^h \gamma U_w \, dn\right). \tag{5}$$

where U_w is the mean flow velocity in the water (i.e. *phase average* in the liquid phase) and W represents an extra normal-to-surface velocity which would be zero if there were no surface layer. [Note that $U_w(n = b) = U$ and $V_w(n = b) = V$].

Formally, this is very similar to that of Hasselmann (1971) valid for a continuous interface [see surface flow term], but it is applied at base of the layer rather than at a mean surface $\overline{\eta}$.

Note that the equation can be regarded as:
either the kinematic B.C. for the flow below $n = b$ for which W must be given,
or as an equation for the conservation of mass inside the layer.

To use the equation as a boundary condition it is necessary to find a suitable closure for the surface flow term

$$\frac{\partial}{\partial s}\int_b^h \gamma U_w \, dn.$$

Closures are required for even more complicated contributions which appear in the dynamic boundary conditions (e.g. terms corresponding to momentum flow in and into the surface layer giving effective stresses).

The toe (2D) or the foot (3D) of the breaker.

For a physically sound representation of the spilling breaker a crucial point is the modelling of the region where turbulence is generated at the free surface. In a 2D description of the flow this is called the 'toe of the breaker'.

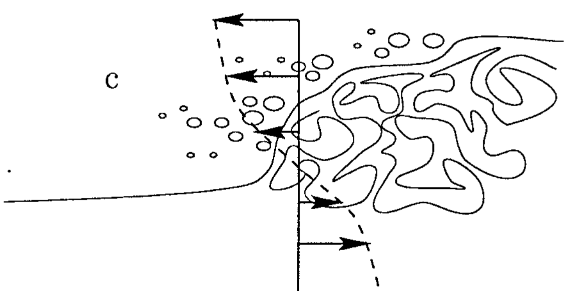

Figure 7: Sketch of the flow and of the velocity profile at the toe of a breaker propagating with celerity c.

According to Peregrine & Svendsen (1978) at the inception point (line) there's meeting of two layers of water travelling in opposite direction. More recently, this scenario has been also reported by Lin & Rockwell, (1995) in their experimental investigation of the early stages of generation of a quasi-steady spilling breaker. In that case, however, since turbulent blobs spill down the wave face (figure 7) generation of turbulence is greater than in a normal mixing layer (where the velocities are in the same direction).

A quantitative description of the inception region has been obtained following the method used by Brocchini & Peregrine (1996) for averaging the flow at the swash zone. Notice that:

- averaging over the turbulence is inadequate in the region right in front of a spiller which the turbulent water only reaches rarely;
- there is little dynamical significance in such a thin intermittent layer of turbulent water;

As a consequence of the above, the whole region which the turbulence only meets intermittently is taken as a 'Boundary Region' (see figure 8) such that there is a non-zero mean depth at the front edge of the layer.

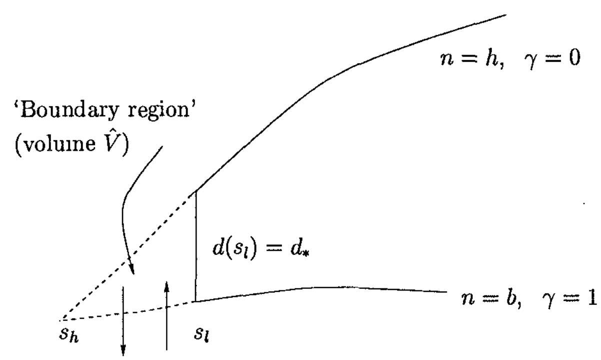

Figure 8: Sketch of the flow properties used in the modelling of the toe of the breaker.

In more detail first introduce the following definitions:

$$d(s_l) = d_* \; ; \qquad d(s_h) = 0 \; ; \qquad h(s_h) = b(s_h) \; ; \qquad \hat{V} = \int_{s_l}^{s_h} d \; ds. \qquad (6)$$

Within our model the toe of the breaker is the mathematical boundary characterized by the coordinate s_l and by a non-zero mean depth d_*.

Following on our illustration based on the equation for the conservation of mass (see Brocchini & Peregrine, 1998b for more details) we integrate the kinematic boundary condition in the streamwise direction from s_l to s_h to get:

$$\frac{\partial \hat{V}}{\partial t} + d_* \frac{\partial s_l}{\partial t} = \left[\int_b^h \gamma U_w \; dn \right]_{s=s_l} - \int_{s_l}^{s_h} \left[\frac{\partial b}{\partial t} + U|_b \frac{\partial b}{\partial s} - V|_b \right] ds. \qquad (7)$$

This equation is formally very similar to one of the shoreline boundary conditions of Brocchini & Peregrine (1996) and it can be regarded as an equation for the motion of the front edge of the layer (s_l) when rewritten as:

$$\frac{\partial s_l}{\partial t} = \frac{1}{d_*}\left\{\left[\int_b^h \gamma U_w \, dn\right]_{s=s_l} - \frac{\partial \hat{V}}{\partial t} - \int_{s_l}^{s_h}\left[\frac{\partial b}{\partial t} + U|_b\frac{\partial b}{\partial s} - V|_b\right] ds\right\} \tag{8}$$

Closure is now needed not only for the surface flow term but also for the volume of water in the 'Boundary Region' $\hat{V}$ and for the mean depth d_*.

Analysis and description of the flow regimes.

In is clear that an in depth analysis of the flow regimes is needed to determine the closures both for the boundary conditions and for the equations relative to the motion of the toe of the breaker. However, analysis of the interaction of turbulence with an air-water interface is interesting *per se* as a large number of natural flows are characterized by strong turbulence at a free surface and they fall in two main classes:

- **turbulence generated at the free surface** (breaking waves, sprays...),
- **turbulence generated far from the surface** (steep rivers, artificial spillways...).

In our description of the flow regimes we assume it is possible to characterize different flow regimes in terms of two flow properties only (Brocchini, 1996; Brocchini & Peregrine, 1997 and Brocchini & Peregrine, 1998a). These are:

1. the turbulence intensity
$$q = \sqrt{2k} \tag{9}$$
where k =turbulent kinetic energy;
2. the length scale L of the most energetic flow feature (wavelength, eddy size, water blob size, ...)

Considering the two stabilising factors of the water surface (gravity and surface tension) four main regions can be found in the (L, q) plane (see figure 9).

For gravity we compare the specific potential energy gL with the specific kinetic energy of turbulence $k = \frac{1}{2}q^2$ and find the Froude number

$$Fr = \frac{q}{\sqrt{gL}}, \tag{10}$$

while for surface tension we compare the specific surface energy $S = T/\rho$ with $\frac{1}{2}q^2L$ to get the Weber number:

$$We = \frac{q^2L}{2S}. \tag{11}$$

Fr_c and We_c have been obtained working on literature data dealing with wave generation, bubble and drop formation... Here we only summarize some of the results which can be found with more detail in Brocchini & Peregrine (1998a).

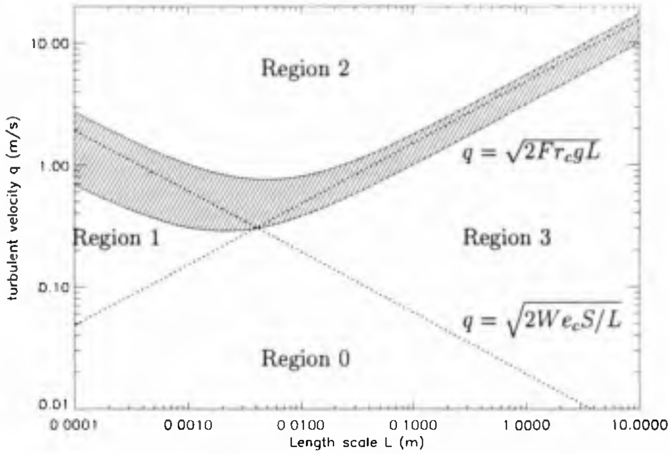

Figure 9: Diagram of the (L, q) plane. The shaded area represents the region of marginal breaking and has been obtained two values for both the critical Weber number $(0.3 < We_c < 5)$ and the critical Froude number $(0.5 < Fr_c < 1.5)$.

Region 0: $Fr \ll Fr_c$ and $We \ll We_c$

In this region the stabilizing effects are dominant leading to a nearly flat surface. Hence, the free surface behaviour in this quadrant may be described as either *flat* or *wavy* (see figure 10).

Figure 10: Illustration of a *flat* or *wavy* surface.

Region 1: $Fr > Fr_c$ and $We < We_c$

For large Froude number and small Weber number we are concerned with relatively small scale turbulence: of the order 1 cm and less for water, region

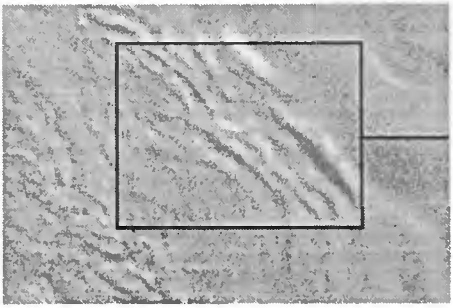

Figure 11: Illustration of a *knobbly* or *microbreaking* surface.

1 of figure 9. Here surface tension is well able to maintain the cohesion of the liquid but gravity fails to keep the surface flat. The result is smooth rounded surfaces. If the turbulence is below the critical region then there is not much wave generation and we describe the surface as *knobbly* or *microbreaking*.

Region 2: $Fr \gg Fr_c$ **and** $We \gg We_c$

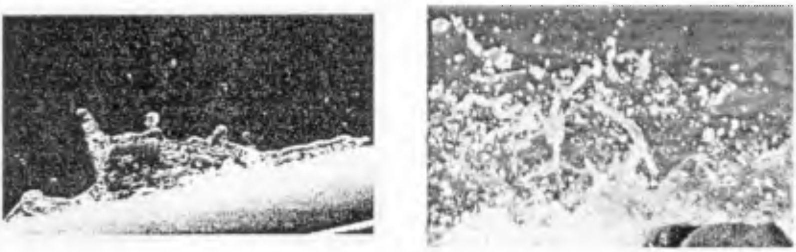

Figure 12: Illustration of a *weakly splashing* surface (left) and of a *violently splashing* surface (right).

When turbulence is so strong that neither surface tension nor gravity can maintain surface cohesion the flow breaks up into drops and bubbles, region 2 of the (L, q) plane. This is an essentially two-phase flow region. At a free surface there is the growth and decay of the strong turbulence to consider as well as the structure of the transition between gas and liquid. When strong turbulence, generated elsewhere, meets a free surface it 'erupts' as the fluctuating eddies form blobs of liquid that are no longer restrained by the inertia of surrounding non-turbulent liquid. This eruption may be exemplified by the 'rooster tail' seen at the rear of high speed vessels as the turbulent flow from their driving mechanism meets the free surface. Sometimes the flow is sufficiently well organised that some of the 'tail' is due to a discrete splash.

We can contrast this case with the weak turbulence case of an almost flat surface. For weak turbulence the vertical velocity fluctuations v approach zero at the free surface, on the other hand for strong turbulence v can be expected to be larger than u and w since the horizontal fluctuations are more constrained by the inertia of the surrounding liquid. This complete contrast in the variation of v gives the clearest indication that different surface regimes need different approaches in developing turbulent models. At the very least different closures are needed for averaged terms.

Region 3: $Fr < Fr_c$ and $We > We_c$

Region 3 of our (L, q) diagram has gravity dominating the turbulence, $Fr \gg 1$, with weak surface tension, $We \ll 1$. It is by far the commonest state since it applies to almost all terrestrial water bodies with flow: stream, rivers, seas and oceans. The free surface is essentially flat or nearly so. Linearised boundary conditions are generally satisfactory. However, there are a range of interesting flow properties in this regime as the turbulent energy is increased towards the splashing case. These are local effects and their significance in various applications is not well determined.

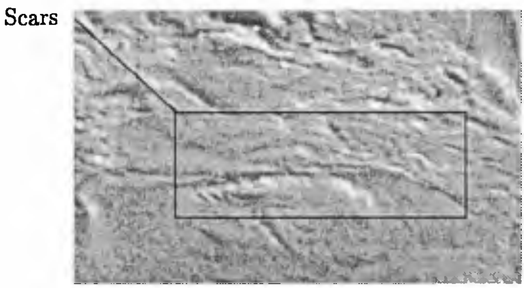

Figure 13: Illustration of a *scarified* surface.

These phenomena arise since the turbulence has more than adequate energy to disturb the free surface, but only at length scales which are smaller than the main turbulent eddies. At the edge of the eddies, where strong shear develops, or where the eddy boundary is moving or there is a strong surface convergence shorter length scales, $L/10$ or $L/100$ or even less becomes important. The surface develops linear features, or scars, which may be a sharp downward trough as shown in figures 4 and 13, or else involve localised breaking.

Acknowledgements

Support from the European Commission Research Grant MAS3-CT97-0081 (SASME) and the Office of Naval Research NICOP Grant N00014-97-1-0791 is gratefully acknowledged.

References

BROCCHINI, M. (1996). *Flows with freely moving boundaries: the swash zone and turbulence at a free surface.* Ph.D Dissertation. University of Bristol, Bristol.

BROCCHINI, M. & PEREGRINE, D.H. (1996). Integral flow properties of the swash zone and averaging. *Jour. Fluid Mech.* **317**, 241-273.

BROCCHINI, M. & PEREGRINE, D.H. (1997). Strong turbulence at a free surface. *Proc. Conf. on Wind-over-Wave Couplings: Perspectives and Prospects*, Inst. Maths. & its Applic. Salford, eds. S.G.Sajjadi & N.Thomas, Oxford Univ. Press. (To appear). Salford.

BROCCHINI, M. & PEREGRINE, D.H. (1998a). The dynamics of turbulent free surfaces. Part 1. Description of strong turbulence at a free surface. *to be submitted.*

BROCCHINI, M. & PEREGRINE, D.H. (1998b). The dynamics of turbulent free surfaces. Part 2. The boundary conditions. *to be submitted.*

COOKER, M.J., PEREGRINE, D.H., VIDAL, C. & DOLD, J.W. (1990). The interaction between a solitary wave and a submerged semicircular cylinder. *Jour. Fluid Mech.* **215**, 1-22.

DREW, D. (1983). Mathematical modelling of two-phase flow. *Ann. Rev. Fluid Mech.* **15**, 261–291.

HASSELMANN, K. (1971). On the mass and momentum transfer between short gravity waves and larger-scale motions. *Jour. Fluid Mech.* **50**, 189–205.

LIN, J.C. & ROCKWELL, D. (1995). Evolution of a quasi-steady breaking wave. *Jour. Fluid Mech.* **302**, 29–44.

PEREGRINE, D.H. (1992). Mechanisms of water-wave breaking. In *Breaking waves. IUTAM Symposium, Sydney.* (ed. M.L. Banner & R.H.J. Grimshaw), 39–53.

PEREGRINE, D.H. & SVENDSEN, I.A. (1978). Spilling breakers, bores and hydraulic jumps. *Proc. 16th Int. Conf. Coastal Eng.* , ASCE, **1**, 540–550.